Electronic supplementary information for

Sample-to-answer centrifugal microfluidic droplet PCR platform for quantitation of viral load

Lidija Malic, ∗‡[a,b,c] Liviu Clime, ‡[a,b] Byeong-Ui Moon,[a,b] Christina Nassif,[a,b] Dillon Da Fonte, [a,b] Daniel Brassard, [a,b] Ljuboje Lukic,[a,b] Matthias Geissler, [a,b] Keith Morton,[a,b] Denis Charlebois,[d] and Teodor Veres[a,b,e]

[a] *Life Sciences Division, National Research Council of Canada, 75 de Mortagne Boulevard, Boucherville, QC, J4B 6Y4, Canada. E-mail: lidija.malic@cnrc-nrc.gc.ca*

[b] *Center for research and application of fluidic technologies (CRAFT) @ NRC and University of Toronto*

[c] *Department of Biomedical Engineering, McGill University, 775 Rue University Suite 316, Montreal, Quebec H3A 2B4*

[d] *Canadian Space Agency, 6767 Route de l'Aéroport, Saint-Hubert, QC, J3Y 8Y9, Canada*

[e] *Department of Mechanical and Industrial Engineering, University of Toronto, 5 King's College Road, Toronto, ON, M5S 3G8*

‡ *These authors contributed equally to this work.*

Contents

1. Pneumatic manifold

The pneumatic module comprises 12 independent pneumatic lines per cartridge. The pneumatic manifold (Fig. S1) comprising 12 pressure outlets, each outfitted by an O-ring, is embedded on the floor of the rotating stage and connects to the openings of the pressure ports (Inlets) positioned on the bottom surface of the cartridge.
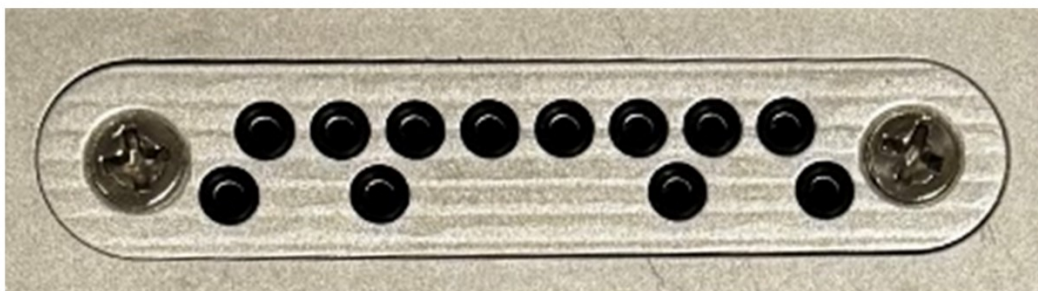

Fig. S1 Photograph of the pneumatic manifold embedded on the floor of the rotating stage. All 12 pressure outlets are surrounded by an O-ring to seal the interface upon contact with the cartridge.

2. Fluidic interface to the PCR tube

The PCR amplification is performed in disposable 200 µL PCR flat cap tubes (Cat. No. TFI0201; Bio-Rad). Transfer of the emulsion to and from the tube is performed using laboratory tubing (Liveo Laboratory tubing, CAT. No 508-003; The Dow Chemical Company, Midland, MI). Three pieces of tubing (1–3), each ~10 cm long, are connected to the cartridge at the 'PCR pressure', 'PCR-to-chip' and 'Chip-to-PCR' ports (Fig. 1a and 2) using PTFE tube connectors and are inserted into the cap of the PCR tube through holes of 1 mm in diameter, as shown in Fig. S2. The holes are then sealed with UV glue (LOCTITE AA 352, part no. 35241; Henkel, Mississauga, ON) on the inner side of the cap. Tubing (1) and (2) are cut short below

the cap while tubing (3) is maintained at the length of the tube to collect the entire volume of the emulsion after PCR amplification. Tubing (3) is also trimmed at an angle to prevent closing in negative pressure mode.
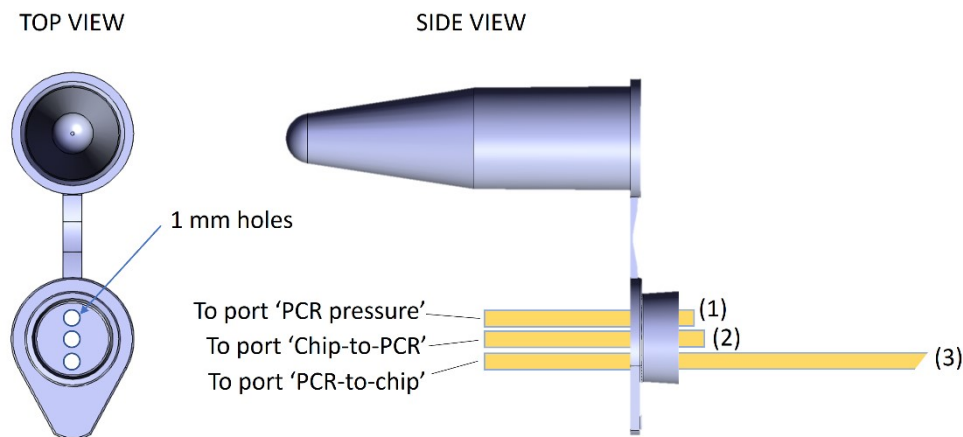

Fig. S2 Fluidic interface at the PCR tube. Schematic showing the positioning of the holes in the tube cap (top view) and the configuration of tubing (side view). The ports 'PCR pressure', 'Chip-to-PCR' and 'PRC-to-chip' on the microfluidic cartridge are indicated in Fig. 2a.

3. Miniature PCR thermocycling module

The miniature PCR thermocycling module is implemented using resistive heating of a standard PCR tube. A Nichrome 28-gauge metallic wire (13.42 Ohms/m; Master Wire Supply) is coiled around the tube (Fig. S3a) for heating and a high-speed miniature electric fan (9000 rpm and 2.5 CFM; WinSinn Technology) is used for cooling (Fig. S3b). The wire and the PCR tube are supported by a 3D printed body fabricated with a precision 3D printer (Phrozen Mini 4K; Phrozen, Toronto, ON) and high-resolution resin (Siraya Tech Build Smoky Black 405 nm; San Gabriel, CA). A negative temperature coefficient thermistor

connected to a microcontroller (Adafruit QT Py ESP32-S2 WiFi; Fig. S3c) is installed at the bottom of the cavity accommodating the PCR tube to be used as feedback by the microcontroller for accurate thermal cycling. The PCR tube is fixed and secured inside the cavity by a detachable cover lid (Fig. S3c) connected electrically to the main body of the module with the help of spring-loaded metallic pads. This lid also comprises an additional heater to prevent condensation on the cap of the PCR tube. A pinch valve mechanism has further been implemented to close the tube completely during PCR thermocycling (see section 4).
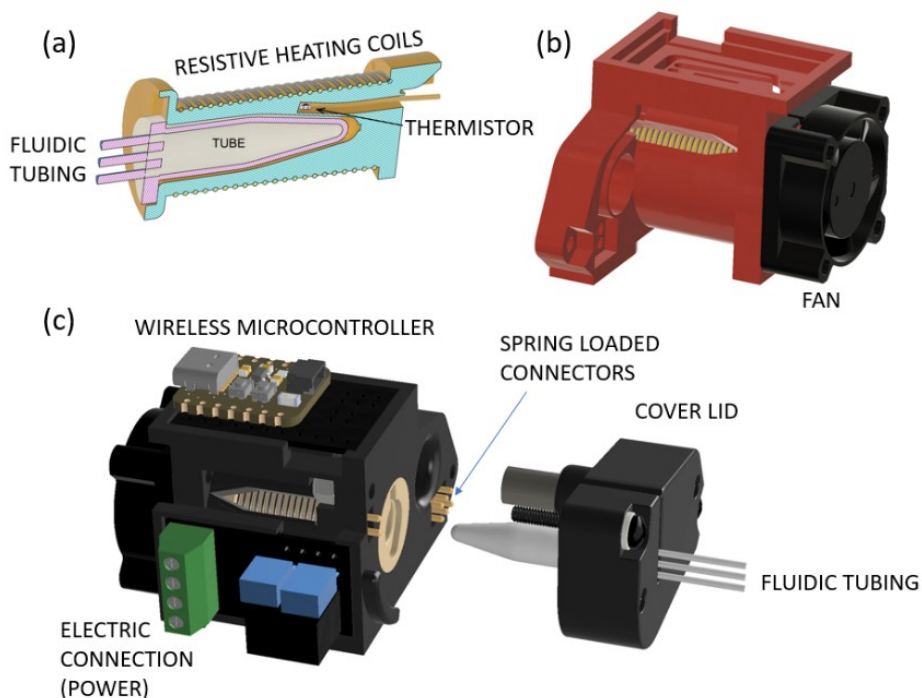

Fig. S3 3D drawings of the miniature PCR thermocycler. (a) Axial cross-sectional area along the symmetry axis of the PCR tube highlighting the resistive heating coil, the thermistor for temperature control, and the fluidic tubing. (b) Main body of the thermocycler with the cooling fan. (c) Complete assembly of the thermocycler consisting of the main body accommodating the PCR tube, the wireless microcontroller, the electric connector and the cover lid with a secondary resistive heating coil for preventing evaporation and a mechanical pinch valve to simultaneously close the fluidic tubing during PCR cycling.

The overall weight of the miniature PCR thermocycler is about 65 g for a size of 60 mm ✕ 55 mm ✕ 42 mm (Fig. S4). The assembled module is mounted on the rotating stage using an adjustable aluminum bracket which places the PCR tube with its symmetry axis on the radial direction of the rotor, and is connected to the 12 V bus provided by the centrifugal microfluidic platform. The cavity in the main body of the thermocycler has a special groove which positions the PCR tube in a unique orientation such that the fluidic tubing is aligned with the slot of the mechanical pinch valve mechanism.

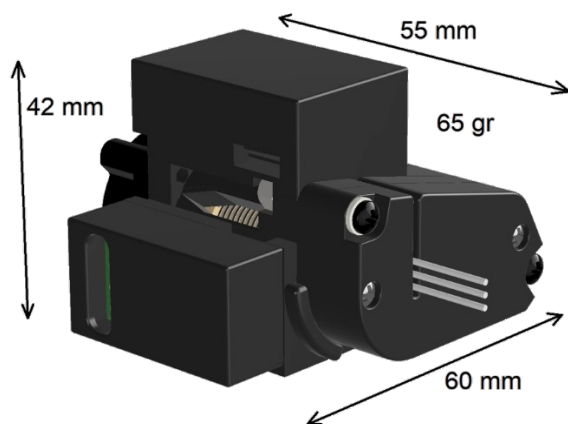**Fig. S4** 3D rendering showing the final assembly of the external PCR module. The arrows indicate the dimensions of the module.

4. Pinch valve mechanism

The thermocycler cover lid comprises a mechanical pinching mechanism that consists of a geared motor rotating an eccentric axle and a 3D printed pinching blade (Fig. S5). The eccentricity of the axle is calculated so that the amplitude of the displacements of the

pinching blade is about 0.8 mm, which is slightly larger than the outer diameter of the silastic tube. In this way, it is possible to close the tube completely, while at the same time making sure that the process is fully reversible. The blade also contains a miniature permanent magnet (1 mm in diameter, 1 mm in length; K&J Magnetics) in the form of an insert which helps control the positioning of the blade through a miniature Hall sensor (Texas Instruments, Dallas, TX) mounted in vicinity on the cover lid.
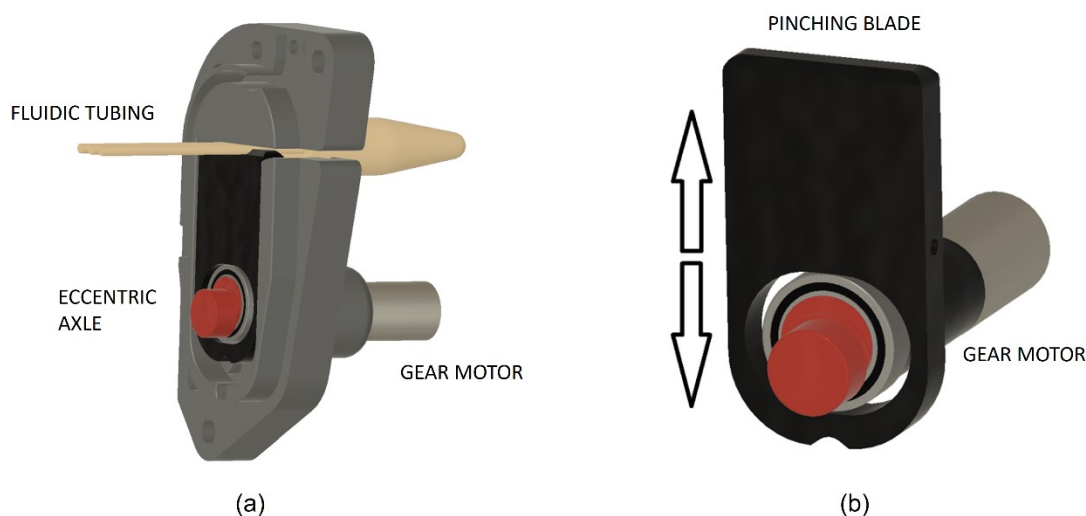
Fig. S5 Pinching mechanism for the miniature thermocycler. (a) 3D model of the unit. A geared motor is rotating an eccentric axle which pushes a pinching blade against the fluidic tubing to (temporarily) cut off connectivity. (b) Close-up view of the pinching blade with the geared motor and the eccentric axle.

5.   Miniature PCR thermocycler: Programming and performance

The temperature control at the hardware level is achieved by using the Arduino (C) programming languages and a PID standard algorithm with the temperature from the thermistor in the thermocycler body used as the main input. The graphical user interface and

the sequencer are programmed in Java. Since the body of the thermocycler is 3D printed (in a material with low thermal conductivity), we might expect that the temperature along the tube is not constant. This implies that the calibration has to be done according to the volume of oil contained in the PCR tube as this affects the positioning of the droplet layer in the tube. In Fig. S6, we give an example of a PCR cycling protocol corresponding to 75 µL of oil in the PCR tube, that is, the droplet layer is approximately at the middle of the tube.
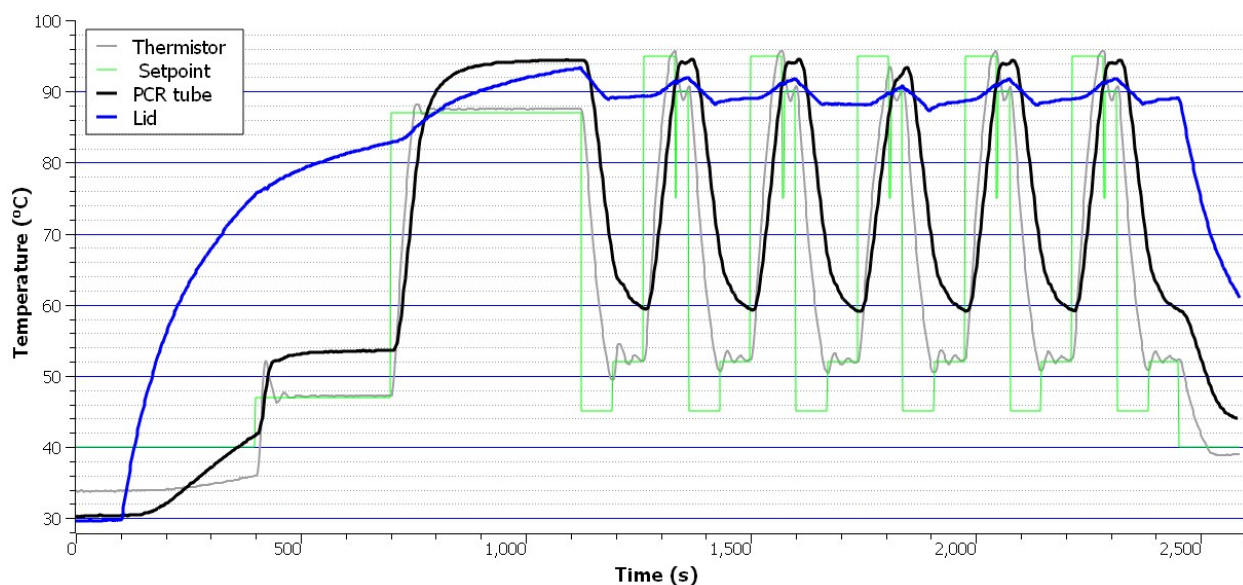
Fig. S6 Temperature measurements for a short PCR protocol (5 cycles) highlighting the temperature setpoint (green), the temperature at the control thermistor (gray), the temperature of the liquid in the PCR tube (black) and the temperature of the PCR tube cap (blue).

Temperature cycling at maximum heating and cooling rates (Fig. S7) indicates average heating and cooling rates of ~ 0.7 °C/s. Experimental measurements of heating/cooling rates (not shown here) suggest that they do not change with the rotation speed of the rotor of the centrifugal microfluidic platform.

Fig. S7 Temperature cycling between 60 and 90 °C at maximum heating and cooling rates. The gray curve represents the temperature measured by the heater's thermocouple. The red curve represents the actual temperature measured inside the PCR tube inserted into the heater.

6.   Miniature epi-fluorescence imaging module
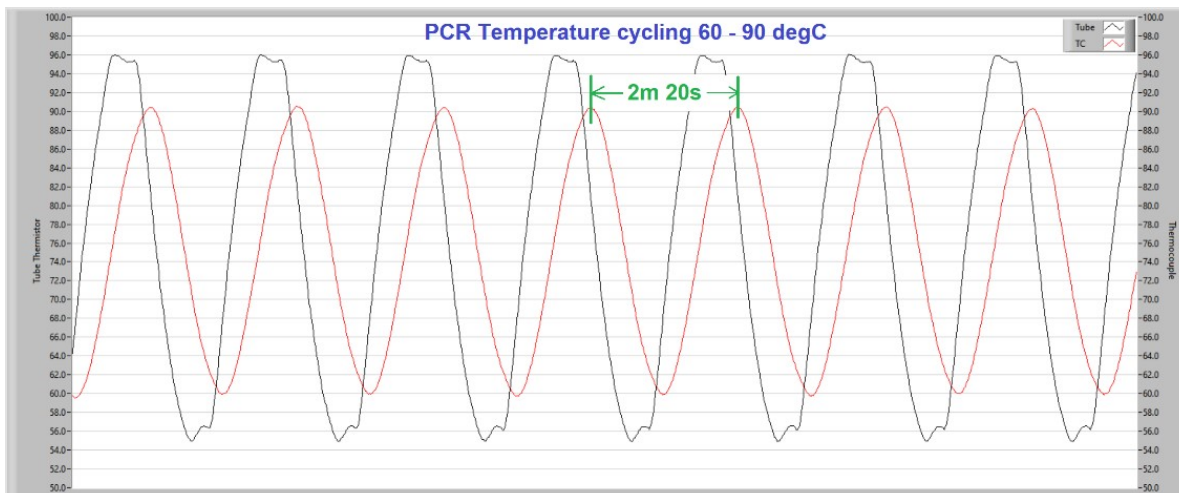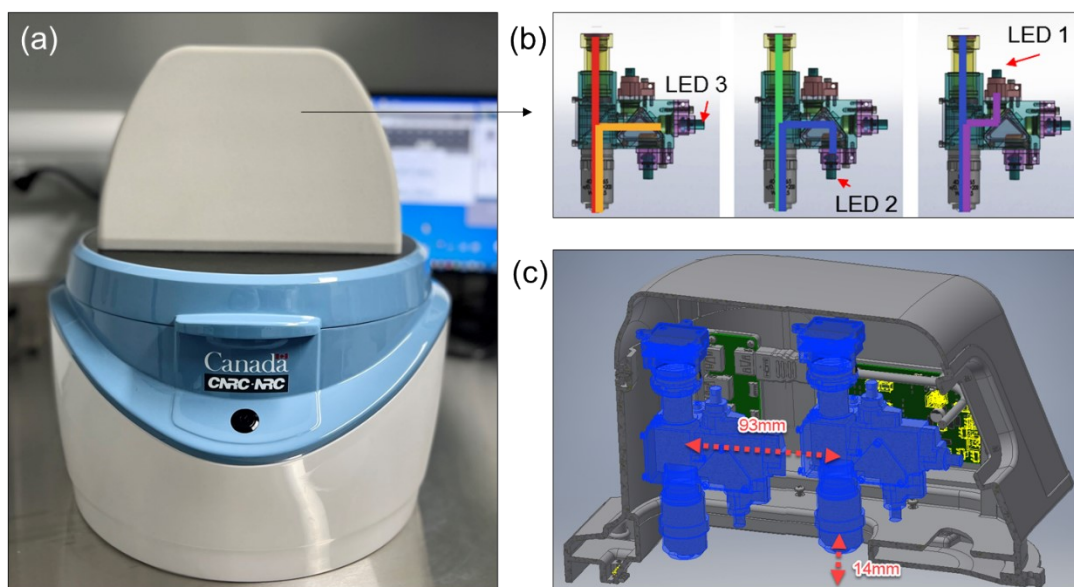

Fig. S8 Miniature fluorescence imaging module. (a) Photograph of the centrifugal microfluidic platform comprising the embedded module (cover lid closed (b) The system features three fluorescence excitation channels at 488 nm, 555 nm, and 645 nm. (c) The imaging module is mounted on a translation stage for precise positioning and focus.

The centrifugal platform is equipped with a miniature epi-fluorescence imaging module mounted inside a custom-built cover lid (Fig. S8). A white LED ring light with custom-made diffuser is used to provide even radial illumination around the objective for brightfield observation. The image acquisition is performed in stationary conditions, such that once the rotor stops at an angular location, the use of the linear translation stage allows for accurate positioning of the objective above the designated area of the imaging chamber, while the vertical translation stage is used for focusing. Once the image is acquired, the vertical stage

retracts the objective to safe position for a subsequent change in location. Using the combination of linear stage movement and angular translation of the rotor, all designated areas of the sample can be covered for observation and image acquisition. The platform is also equipped with a stroboscopic imaging system comprising a triggered USB camera (PL-D721CU-T; Pixelink, Ottawa, ON) for real-time visualization of the on-chip process.

7. Design of the imaging chamber

Initially, the bottom part of the imaging chamber (I) is filled with oil (in excess) to ensure wetting and unhampered transition of the emulsion from the top part. To bring down droplets into the imaging chamber, negative pressure is applied to ports #8 and 12. In this way, oil is gradually extracted from the bottom of the chamber, forcing the droplets to slowly enter the shallow region and form a monolayer (Fig. S9). The slow process of monolayer formation is implemented to minimize the risk of droplet merging. The imaging chamber (I) has been positioned slightly off the median line of the cartridge (Fig. S10) to ensure that the chamber is properly filled with droplets. As the oil is extracted from the imaging chamber, the free surface at the interface between the oil and the emulsion evolves continuously from the L1 to the L2 isobars for the droplets to arrive first at the corner A of the chamber and then at the corner B. In other words, the distance between the corner B and the median line has to be larger than the distance between the corner A and the same median.
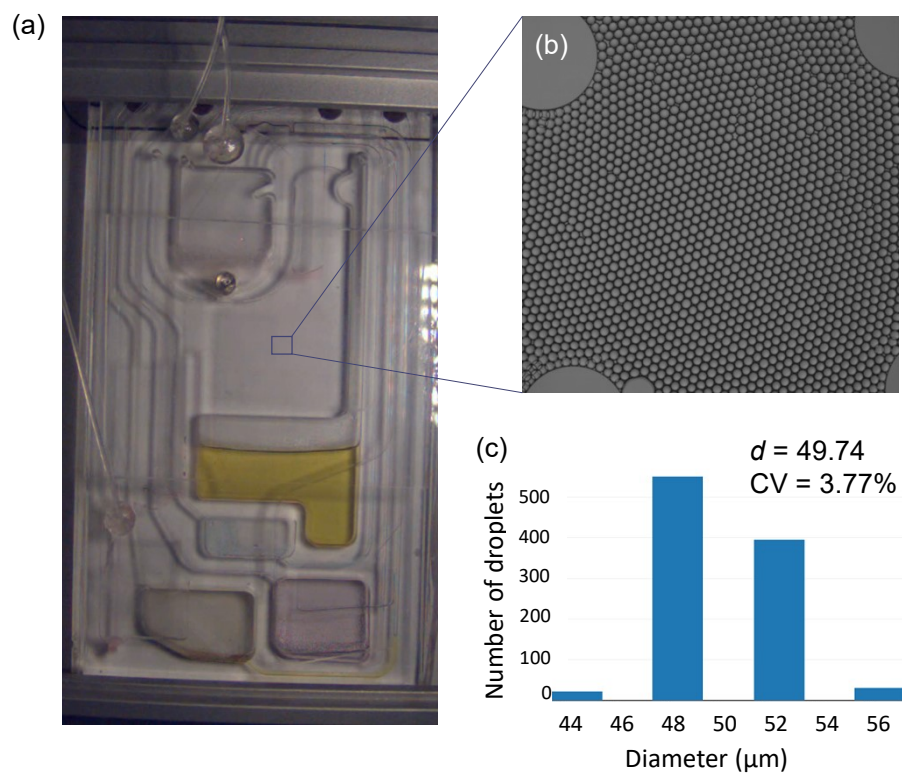
Fig. S9 (a) Stroboscopic image of the cartridge during transfer of the emulsion from the PCR tube into the imaging chamber. (b) Optical micrograph of a close-packed droplet monolayer within the lower segment of the imaging chamber. (c) Plot of droplet size distribution as obtained from image analysis.
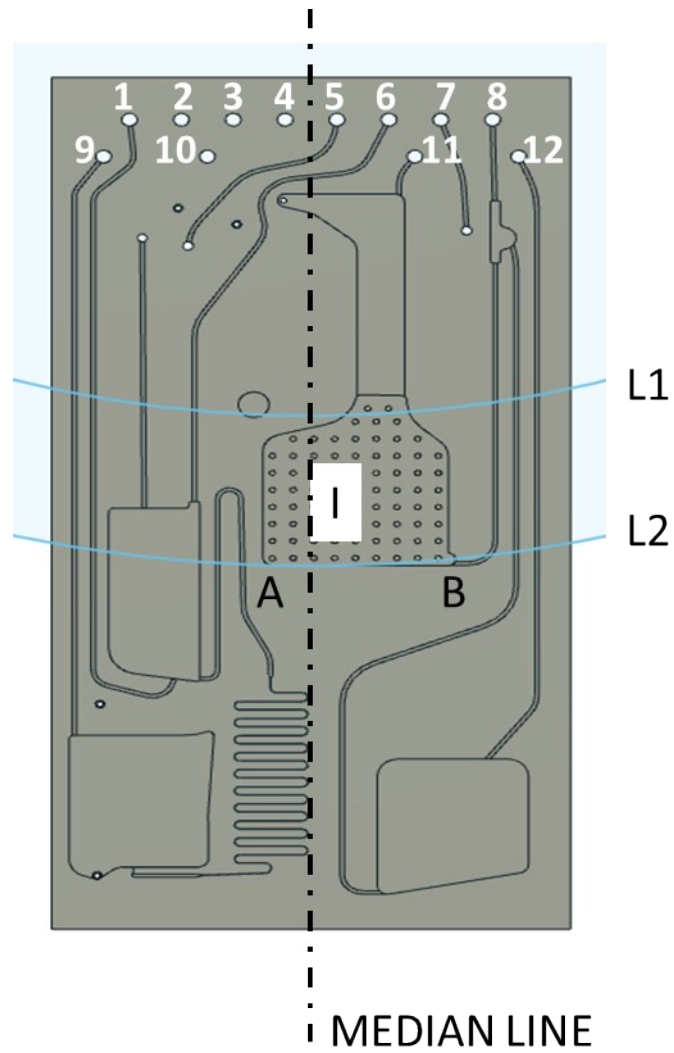
Fig. S10 Schematic of the droplet generation microfluidic device highlighting the positioning of the imaging chamber (I) with respect to two isobars L1 and L2. The shallow portion of the chamber is populated with circular support posts to minimize deformation.

14

8.   Dimensions of microfluidic features

Table S1 Critical dimensions of microfluidic design elements

Microfluidic feature	Size
Bottom channels	40 µm in width, 40 µm in depth
Bottom reservoirs	4.5 mm in depth
Top reservoirs	1.02 mm in depth
Imaging chamber	60 µm in depth
Top channels	40 µm in width, 40 µm in depth
Serpentine channel	50 µm in width, 30 µm in depth
Nozzle channels	15 µm in width, 10 µm in depth
Terrace	52 µm in length, 30 µm in height

Table S2 Reservoirs implemented in the microfluidic design

| Reservoir #	Purpose	Location on cartridge	Capacity (µL)	Assay component	Input volume (µL)
1	Sample/lysis	Bottom level	670	Sample + lysis buffer	175
				binding buffer	100
2	RNA extraction	Bottom level	980	Sample/lysis/binding	275
3	Wash	Bottom level	710	Wash buffer	600
4	Elution	Bottom level	85	Elution buffer	25
5	Waste	Bottom level	1830	n/a	n/a
6	PCR mix	Top level	140	PCR master mix + eluted RNA	50 + 25
7	Oil	Top level	170	Fluorinated oil	100
8	Droplet generation	Top level	170	Oil + generated droplets	70 + 75
9	Droplet imaging[a]	Top level	15 + 105	Oil + emulsion	15

[a] The droplet imaging chamber comprises a deep upper compartment for emulsion transfer and a shallow lower portion for droplet imaging.

9.   Fabrication of all-thermoplastic microfluidic cartridge

We have developed a process to demonstrate that microfluidic devices can be fabricated entirely from thermoplastic materials as a potential path towards generating a single, monolithically integrated consumable (Fig. S11). The device design included both micro-scale droplet generating structures alongside much larger reservoirs and channels for reagent storage and sample processing. To monolithically integrate these disparate micro- and macrostructures, we implemented a hybrid approach that initially uses hot embossing to fabricate the microscale features, followed by CNC machining of macroscale channels and reservoirs. Critically, the CNC machining step is aligned to the as-embossed microstructures for which a custom, camera-based vision system was developed. CNC micromachining circumvents the relatively long processing times (days) required for implementation of very deep fluidic features (>100 μm) using photolithography. The hybrid CNC approach also allows for seamless design modifications, enabling significant flexibility to quickly optimize fluidic handling on the centrifugal platform. The complete fabrication process is detailed below.

Master molds for the hot embossing step were made by sequential photolithographic patterning of multiple layers (10, 30, and 50 μm thick) of SU-8 photoresist (Gersteltec, Pully, Switzerland) spin coated onto chrome-coated 150 mm diameter glass wafers. We used back side exposure of the SU-8 through the glass wafer and a photolithography patterned chrome layer to ensure positive side wall draft angles in the final microstructured channel and

reservoir mold elements fabricated in the SU-8 resist layers. Photopatterned SU-8 resist exhibits a slight undercut in the final patterned features when exposed from the top side due to the attenuation of the UV radiation through the thickness of the resist. While this is not typically problematic for replication and demolding of elastomeric materials (such as PDMS), hot embossing into hard, thermoplastic materials demands for facile separation, and mold durability depends critically on carefully controlling wall draft angles on the working molds. We created positive side wall draft angles in each of the SU-8 photoresist layers by exposing them through a photolithography-defined, opaque chrome layer. The glass wafers were first sputter-coated with 100 nm of chrome (CMS-18; Kurt J. Lesker,) and then spin coated with positive AZ 3312 photoresist (2000 rpm; Integrated Micro Materials, Argyle, TX). Following photolithography and development (EVG 6200; EV Group, St. Florian am Inn, Austria), the exposed areas of the chrome thin film were dissolved with aqueous Cr-7 etchant (Sigma-Aldrich). This patterned chrome layer on the glass substrate includes all the microstructured elements for each of thicker, 30 and 50 μm SU-8 layers that will be defined by back side exposure. Note also that fiducial alignment marks for the future CNC machining step were included as well to facilitate the alignment of the CNC toolpath to the as-embossed features (Fig. S11). After removing the remaining AZ 3312 photoresist, cleaning and drying the glass substrate, a ~1-μm-thick adhesion layer (SU-8 1040, 4600 rpm) was spin coated directly onto the micropatterned chrome layer. This layer was crosslinked by top side flood exposure. Next, a 10-μm-thick resist layer (SU-8 1060, 2400 rpm) was spin coated onto the adhesion layer and crosslinked using standard top side photolithography in conjunction with a chrome photomask. Each SU-8 photoresist layer step described here includes an initial, 3 s pre-spin at 500 rpm followed by standard temperature and time ramps on a

programmable hot plate (HS40A, Torrey Pines Scientific, Carlsbad, CA) for all pre-bake, post-exposure bake, and hard bake steps. PGMEA (Sigma-Aldrich) was used to develop each SU-8 resist layer. The small array of 8 parallel, 15-µm-wide, droplet generation nozzles are the only features defined in this first 10-µm-thick SU-8 layer and side wall undercut is not problematic for these shallow features. Following patterning and development of the droplet generation nozzles, the 30-µm-thick resist layer for the serpentine channel was spin-coated directly over the patterned 10 µm layer (SU-8 1060, 850 rpm) and crosslinked by back side flood exposure through the glass wafer and the patterned chrome layer. Prior to exposure, the clear areas of the pre-patterned chrome layer associated with the 50 µm layer were temporarily masked off using black tape applied to the back of the glass substrate. No alignment is necessary during this step because the chrome photomask is embedded under the resist stack. Finally, the 50 µm layer in which the droplet visualization chamber is defined was spin-coated (SU-8 1070, 1550 rpm) on top of the 30 µm layer. Here again, alignment-free back side flood exposure was used to crosslink this last layer and black tape applied to the back of the glass substrate was use to mask off clear areas associated with the previous 30 µm thick layer features. Following development and hard bake of this final microstructured layer, the wafer was cleaned and silanized using trichloro(1H,1H,2H,2H-perfluorooctyl)silane (Sigma-Aldrich) under vacuum in a glass bell jar.

Working molds for hot embossing were made by first replicating the multi-level SU-8 mold masters using PDMS (Sylgard 184) mixed thoroughly (DAC 250 Speedmixer; FlackTek, Landrum, SC) with a 10:1 (wt./wt.) ratio of elastomer base and curing agent. Following degassing under vacuum, the PDMS is cured at 80 °C for a minimum of 2 h in a custom jig. After demolding, this PDMS replica is used to create a working stamp for hot

embossing. We fabricate the working stamp by UV crosslinking of Fluorlink MD700 Darcour 1174; BASF, Ludwigshafen, Germany) on a 150 mm diameter glass substrate. A primer (X-40-9271; Shin-Etsu Chemical, Tokyo, Japan) applied to the glass substrate is used to promote adhesion between the fluoropolymer and the glass substrate during the UV curing step.

Blank Zeonor 1060R polymer substrates (175 mm in diameter, 4 mm in thickness; Microfluidic ChipShop, Jena, Germany) were hot embossed (EVG 520; EV Group) using the fluoropolymer working stamps which usually featured two device footprints per substrate. The plastic substrates were embossed at 145 °C with an applied force of 15 000 N for 6 min following a temperature ramp-up and 10 min hold under 700 N applied force. Following hot embossing, the as-embossed polymer substrates were mounted in a custom chuck on the CNC machine for zeroing and tool path alignment to the fiducial alignment marks included with the embossed microstructures. CNC machining was used to create interconnected pneumatic lines and ports, fluidic channels, reservoirs and through-hole vias on both sides of the device. Alignment of the CNC tool path to the as-embossed microstructures using the vision system and embossed marks enables sub-50 μm precision between CNC defined features and microstructured elements. Once embossing and CNC machining are completed, the cartridge is enclosed on both sides using cover substrates produced by laminating a thermoplastic elastomer sheet (223 μm in thickness; Gel-Pak, Hayward, CA) to Zeonor ZF-14 (188 μm in thickness; Zeon Corporation, Tokyo, Japan). The sheets are then cut to size. Holes for pressure ports are punched manually in the cover substrate prior to assembly.
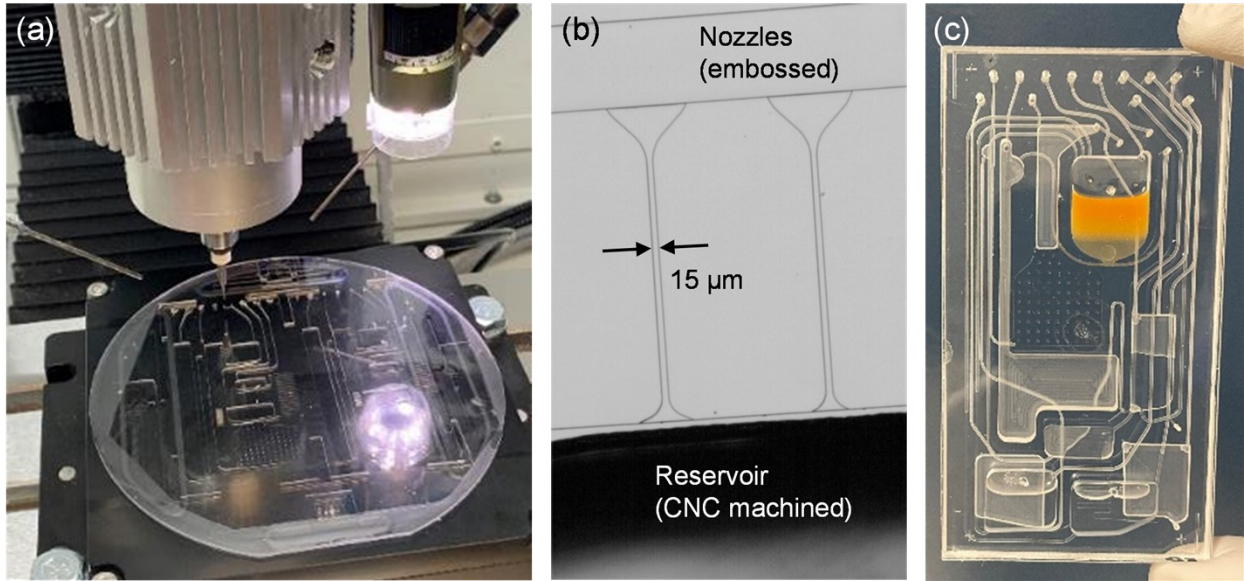
Fig. S11 All-thermoplastic microfluidic cartridge. (a) Photograph of the CNC machining process used to create interconnected pneumatic lines and ports, fluidic channels and reservoirs, and through-hole vias on both sides of the device. (b) Optical micrograph showing a close-up view of the embossed droplet generation nozzle entering the CNC machined reservoir. (c) Photograph showing an assembled all-thermoplastic cartridge filled with reagents required for the assay.

10. Primers and probes

Table S3 Primers and probes used for RT-qPCR and ddPCR

Gene	Primer/Probe	Sequence (5′ → 3′)	Source
N	Forward	TTA CAA ACA TTG GCC GCA AA	CDC ROU 2019-nCoV_N2
	Reverse	GCG CGA CAT TCC GAA GAA	
	Probe	ROXN-ACA ATT TGC CCC CAG CGC TTC AG-3IAbRQSp	
E	Forward	ACA GGT ACG TTA ATA GTT AAT AGC GT	E_Sarbeco_R2
	Reverse	ATA TTG CAG CAG TAC GCA CAC A	
	Probe	FAM-ACA CTA GCC /ZEN/ ATC CTT ACT GCG CTT CG-3IABkFQ	
RNase P	Forward	AGA TTT GGA CCT GCG AGC G	CDC ROU RNase P
	Reverse	GAG CGG CTG TCT CCA CAA GT	
	Probe	Cy5-TTC TGA CCT /ZEN/ GAA GGC TCT GCG CG-3IABkFQ	

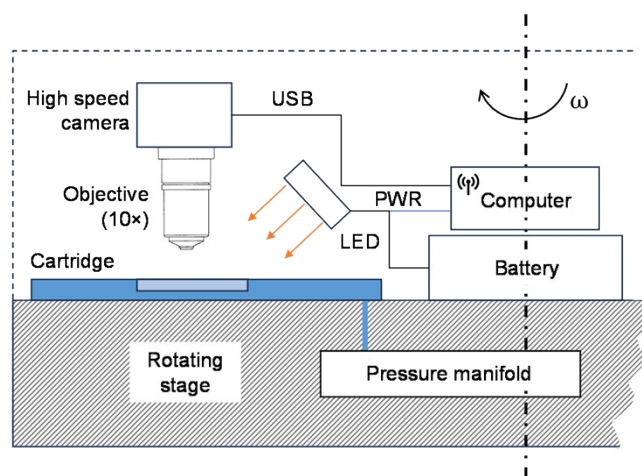# 11. Recording of droplet generation process

Fig. S12 Schematics of the experimental setup used for visualization of the centrifugal step emulsification process.

12. Workflow implementation

The automated workflow implemented on the centrifugal platform (Fig. S13 and Table S4) is preceded by manual loading of buffers and reagents into their respective reservoirs using a micropipette before the cartridge is installed on the platform. The sample (in lysis/binding buffer) is initially introduced in a dedicated reservoir (A) downstream of the RNA extraction chamber (B). This prevents wetting and pre-mature priming of the transfer channel due to the presence of ethanol in the solution which would lead to contamination of the ddPCR master mix in chamber (F). Once the platform starts rotating (e.g., at 400 rpm), the combined sample/buffer mix is transferred to the RNA extraction chamber (step 1). Bubble-induced agitation[22,25] is used to re-suspend and distribute MNPs evenly in the liquid phase (step 2a).

Subsequently, the sample is incubated for 5 min at room temperature to mediate lysis and binding of RNA to the MNPs (step 2b). The rotation speed is then increased to 600 rpm to facilitate capture of MNPs in the region below the permanent magnet (step 2c). The RNA-depleted lysate is transferred to the waste reservoir by applying negative pressure (−0.8 psi) to port #7 (step 3). Two consecutive wash steps are subsequently performed to clean the captured MNPs from buffer residues. The rotation speed is reduced to 400 rpm to facilitate transfer of wash buffer from reservoir (C) located at the bottom of the cartridge. Low positive pressure (e.g., 2 psi) is applied at port #3 (step 4a) such that half of the initial volume is engaged during each wash step. With the magnet in place, incubation is maintained for 5 min to ensure effective removal of non-specifically bound contaminants (step 4b), followed by transfer of the buffer to the waste (step 4c). Similarly, the second wash step is then performed (step 5) to remove remaining residues which could potentially inhibit or interfere with the subsequent ddPCR assay. Upon transfer of the wash solution to waste (step 5c), negative pressure is maintained at port #7 for 1 min (step 6) to evaporate ethanol from the wash buffer and dry the MNPs. Elution buffer is subsequently transferred by activating port #10 (step 7) at low rotation speed. The MNP pellet is re-suspended in the elution buffer using bubble-induced agitation (step 8a), followed by 5 min magnetic capture and incubation (step 8b). The RNA eluted from the beads is then transferred to the PCR mix by activating ports #2, 3, 5, 7, and 10 (step 9) and dispersed using bubble mixing (step 9b). The droplets are subsequently generated by applying positive pressure (i.e., 3.5 psi) simultaneously at ports #1, 2, 3, 5, 6, 7, and 10 (step 10), pushing the liquid through the resistive serpentine channel into the droplet generation unit. Upon completion of the droplet generation process, the rotation speed is reduced and port #9 is activated by successively increasing the pressure

from 2.5 to 3.5 psi to gently transfer the emulsion into the PCR tube (step 11). Following thermal cycling (step 12), the emulsion is transferred into the visualization chamber on the cartridge, enabled by applying positive pressure to the PCR tube (ports #4 and 9). Initially, the bottom part of the imaging chamber is filled with oil (step 13) to ensure wetting and unhampered transition of the emulsion. The droplet transfer from the PCR tube is then performed by activating ports #4 and 9 and successively increasing the pressure from 2.5 to 3.5 psi (step 14). To lower the droplets into the imaging chamber (I), negative pressure is applied to ports #8 and 12 to gradually extract the fluorinated oil from the chamber (step 15). As the oil is withdrawn, the droplets descend into the lower, shallower portion of the chamber (Fig. S9a and S10). The pressure is slowly decreased until the monolayer formation is complete. Finally, the platform is brought to a standstill for image acquisition.

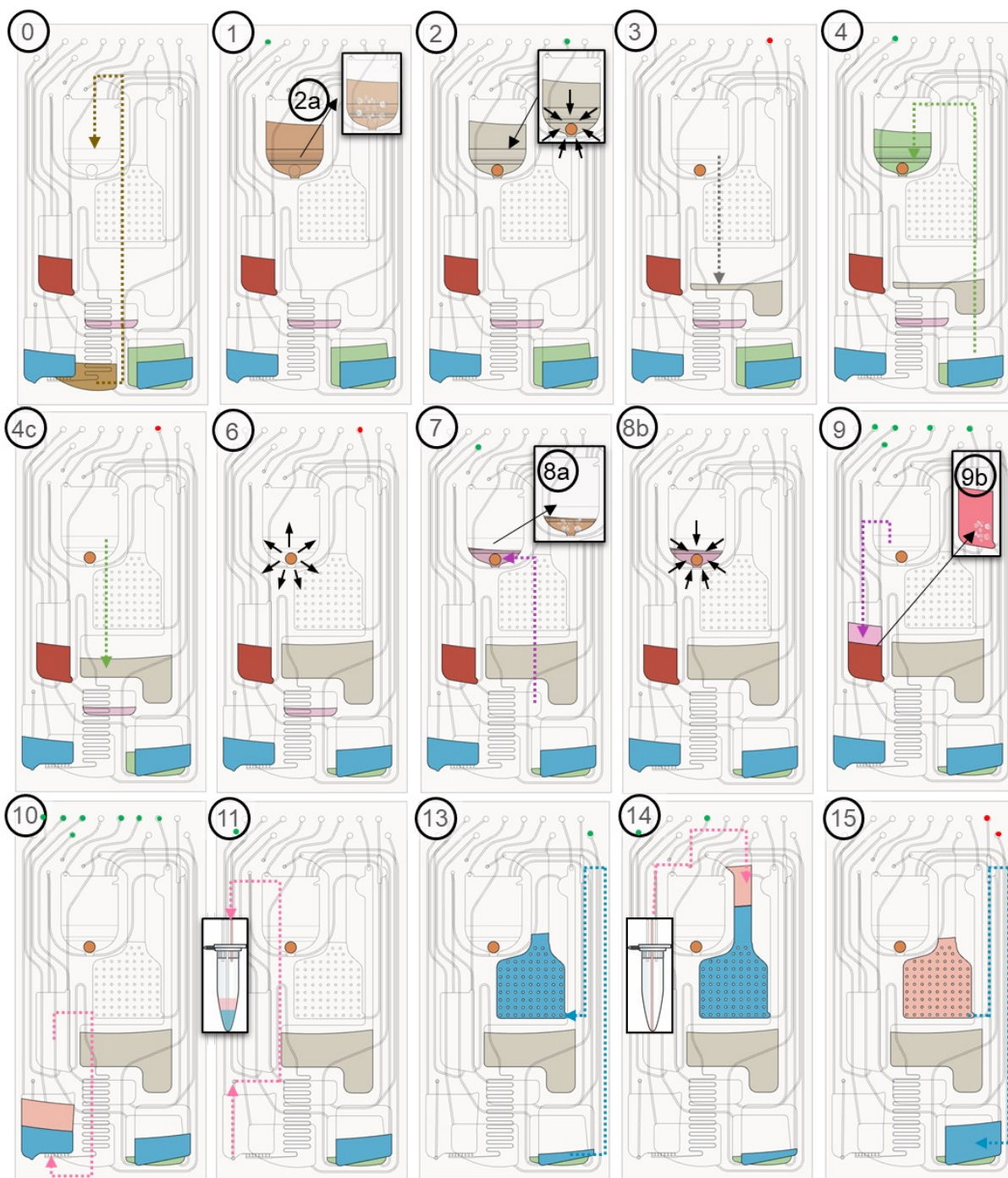**Fig. S13** Schematics illustrating the displacement of liquid on the cartridge during different stages of the process. Arrows indicate the direction of flow; activated ports are highlighted in green or red, representing the application of positive or negative pressure, respectively. A video recording of the actual sample-to-answer workflow using colored solutions is provided as a separate file to the ESI.

25

Table S4 Microfluidic protocol[a]

Step	Operation	Active ports	Applied pressure (psi)[b]	Rotation speed (rpm)	Duration
1	Transfer sample + lysis buffer and MNPs	2	2.6	400	30 s
2a	Bubble mixing of sample and MNPs	7	0.5	600	0.2 s (10 ×)
2b	Incubation (lysis)	–	–	400	5 min
2c	Capture of MNPs	–	–	600	5 min
3	Transfer of lysate to waste chamber	7	–0.8	600	1 min
4a	Transfer of wash buffer (half)	3	2.0	400	30 s
4b	Incubation	–	–	400	2 min
4c	Transfer of wash buffer to waste chamber	7	–0.8	600	1 min
5a	Transfer of wash buffer (remaining half)	3	2.0	400	30 s
5b	Incubation	–	–	400	2 min
5c	Transfer of wash buffer to waste chamber	7	–0.8	600	1 min
6	Air dry of MNP pellet	7	–0.8	600	1 min
7	Transfer of elution buffer	10	1.8	400	10 s
8a	Bubble mixing of elution buffer and MNPs	7	0.5	600	0.2 s (30 ×)
8b	Capture of MNPs	–	–	600	5 min
9a	Transfer of eluted RNA sample to PCR chamber	2, 3, 5, 7, 10	0.8	600	5 s
9b	Bubble mixing of eluted RNA and PCR mix	1	0.5	600	0.2 s (10 ×)
10	Droplet generation	1, 2, 3, 5, 6, 7, 10	3.5	500	45 min
11	Transfer droplets to external PCR tube	9	2.5 to 3.5	300	3 min
12	Thermal cycling[c]	–	–	400	2 h
13	Fill the imaging chamber with oil	12	2.5	340	30 s
14	Transfer droplets from external PCR tube to cartridge	4, 9	2.5 to 3.5	300	5 min
15	Monolayer droplet formation in imaging chamber	8, 12	–0.25	300	3 min
16	Florescence image acquisition	–	–	0	10 min

[a] All steps are performed at room temperature except for the step 12 (thermal cycling). [b] Values are relative to atmospheric pressure. [c] See Experimental section for details.
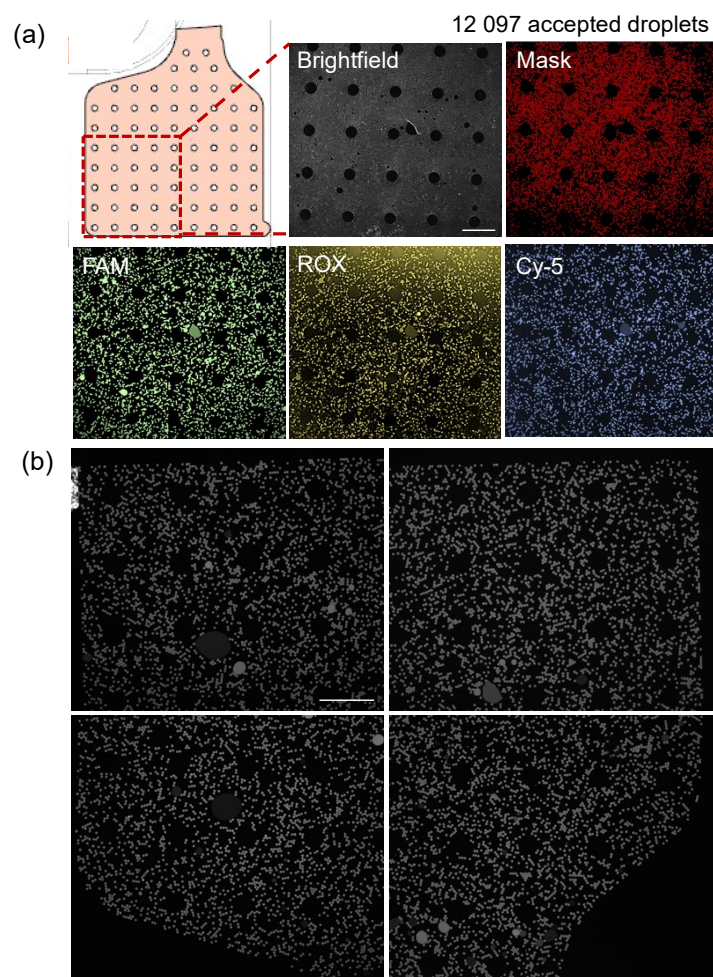
13. Assay validation

Fig. S14 Full field-of-view micrographs acquired using the miniaturized fluorescence imaging system showing amplified droplets of a positive COVID-19 clinical sample following the on-chip ddPCR process. (a) Selected region of the imaging chamber along with the corresponding brightfield, mask and fluorescence images. The typical number of accepted droplets for a single image displayed in the mask (shown in red) that meet the specified size and shape requirements and are used for subsequent fluorescence image analysis is greater than 10 000. In total, for four images that cover the entire area of the imaging chamber, approximately 40 000 droplets are analyzed. (b) Selected micrographs showing typical fluorescence images that are acquired and analyzed with the software for the four non-overlapping regions of the imaging chamber to obtain total droplet counts. The scale bars denote 1 mm.
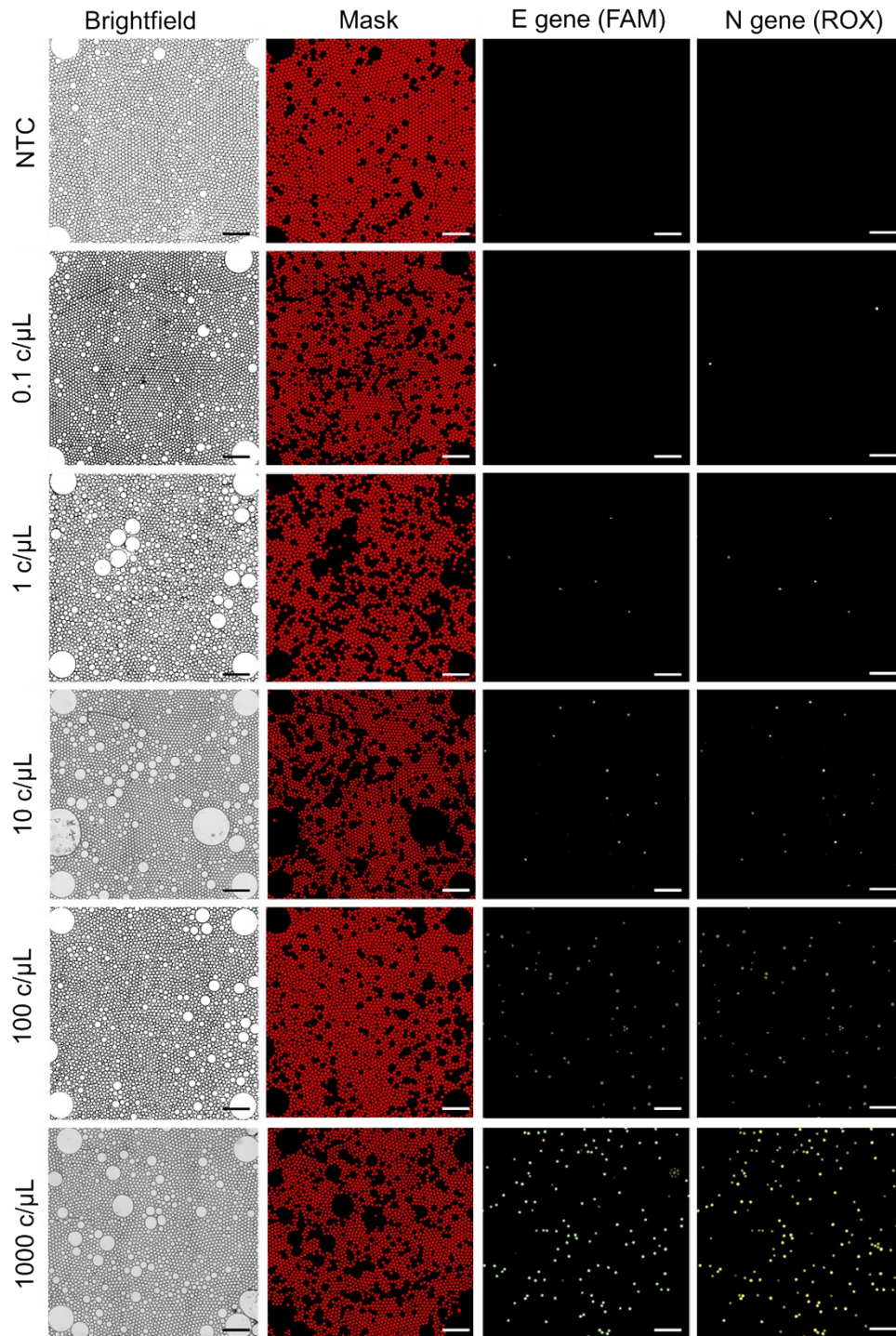
Fig. S15 Brightfield and fluorescence images showing droplet monolayer within the imaging chamber. Here, ddPCR has been conducted using synthetic SARS-CoV-2 RNA diluted in VTM at a concentration of 0.1 to 1000 c/µL. For clarity, only a zoomed-in portion of the imaging chamber is shown to increase visibility of droplets. The scale bars in the images are 400 µm.
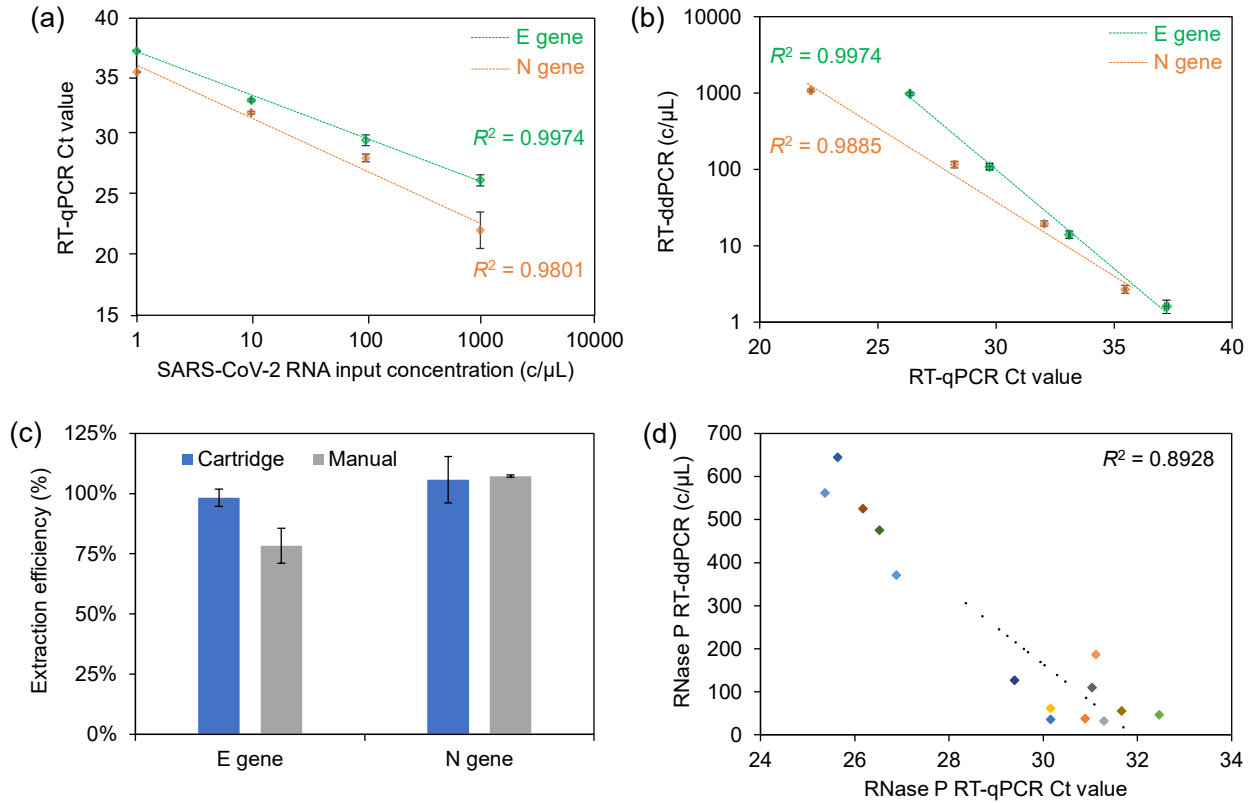
Fig. S16 (a) RT-qPCR titration curves for N and E genes obtained using manually extracted synthetic SARS-CoV-2 spiked in VTM at different concentrations (*n* = 3). (b) Plot comparing viral loads measured by the ddPCR platform to the RT-qPCR Ct values (*n* = 3). (c) Plot of efficiency for on-chip and manual RNA extraction using synthetic SARS-CoV-2 RNA at an input concentration of 100 copies/µL spiked in VTM (*n* = 3). (d) Quantification of on-chip RNA extraction for control gene RNase P using 14 NPS samples from COVID-19 patients and correlation with RT-qPCR Ct values.

Table S5 Summary of analytical results from 14 patient samples

Patient sample ID	Supplier PCR diagnostic test result	Supplier RT-qPCR Ct values (N/E)[a]	RT-qPCR Ct value (N)	SD[b] (N)	RT-qPCR Ct value (E)	SD (E)	RT-qPCR Ct value (RNase P)	SD (RNase P)
N1	Negative	n/a	n/a	0	n/a	0	30.16	0.04
N2	Negative	n/a	n/a	0	n/a	0	30.89	0.04
N3	Negative	n/a	n/a	0	n/a	0	31.28	0.09
P1	Positive	42.00	n/a	0	n/a	0	30.16	0.12
P2	Positive	39.00	39.45	0.37	n/a	0	26.88	0.07
P3	Positive	39.00	38.87	0.26	n/a	0	26.88	0.07
P4	Positive	37.00	38.58	0.47	n/a	0	29.39	0.19
P5	Positive	35.00	36.34	0.30	n/a	0	29.42	0.17
P6	Positive	32.20	33.76	0.52	35.88	0.40	31.03	0.09
P7	Positive	26.40	31.03	0.09	33.35	0.01	31.67	0.07
P8	Positive	23.81	26.13	0.04	27.51	0.03	31.12	0.10
P9	Positive	23.00	24.63	0.09	26.88	0.15	25.63	0.13
P10	Positive	19.88	24.23	0.09	25.94	0.00	26.52	0.02
P11	Positive	18.29	23.09	0.01	24.48	0.09	25.37	0.02

[a] N or E gene non-specified. [b] SD = standard deviation.

14. Technology comparison

Table S6 Summary of selected digital assays conducted on centrifugal platforms

Technology	Number of partitions	Sample-to-answer capacity	Hands-on steps	Throughput (reaction/run)	Sample turnaround time (min)[a]	Limit of detection (copies/µL)	Organization	Ref.
Centrifugal ddPCR	>40 000	Yes	1	2	220	0.1	National Research Council	This work
Centrifugal droplet RPA	800	No	3	1	>30	100	Hahn-Schickard	15
Centrifugal ddPCR	>500	No	4	1	>70	5	Hahn-Schickard	16
Centrifugal ddMDA	Not specified	No	3	6 to 48	>300	1	Xiamen University	17
Centrifugal ddLAMP	Not specified	No	3	2	>90	10	Shanghai Institute of Microsystem and Information Technology	18
Centrifugal ddPCR	35 000	No	4	12	>90	35	Hahn-Schickard	20
Centrifugal ddLAMP	176 000	No	2	1	>35	1	Hahn-Schickard	21

[a] Sample turnaround time is directly dependent on the choice of the NA amplification strategy used. Isothermal amplification assays such as LAMP are typically conducted at a single temperature (e.g., 65 °C), and completed within 30 min, while PCR-based techniques require thermal cycling for a typical duration of 1–2 h.